Supplemental data. De Bianchi et al. (2008). Minor antenna proteins CP24 and CP26 affect the interactions between Photosystem II subunits and the electron transport rate in grana membranes of *Arabidopsis*.

Supplemental Figure 1. **Micrograph of negatively stained grana partition preparation obtained by limited α-DM solubilization of stacked thylakoids.** WT and mutants yielded circular membrane patches of similar shape and size consistent with the diameter of grana stacks as observed in figure 2. The bar is 50 nm.

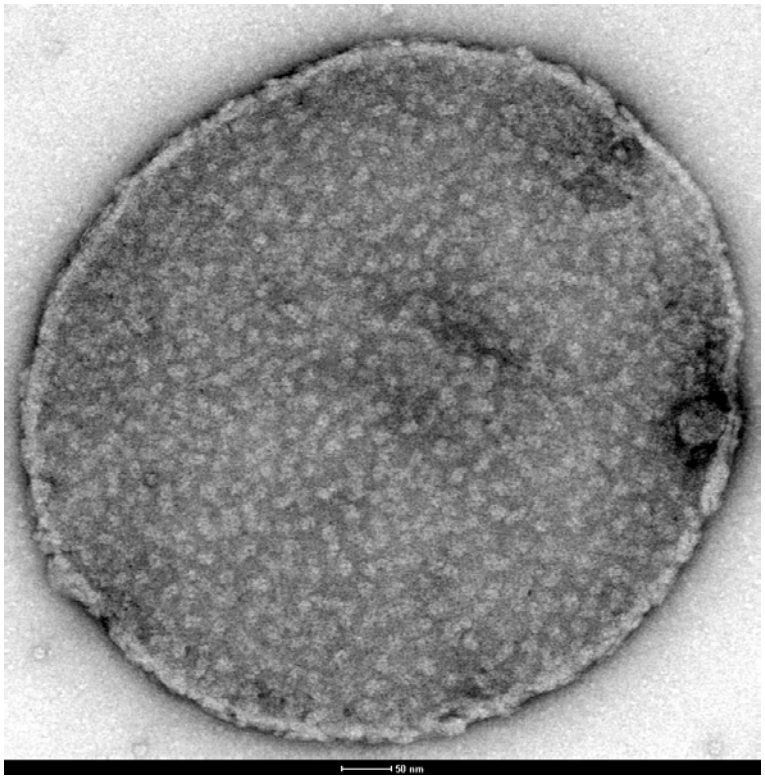

Supplemental Figure 2. Analysis of pigment-protein complexes of WT and mutant. Pigmented complexes from thylakoids and BBY were separated by denaturing SDS-PAGE.

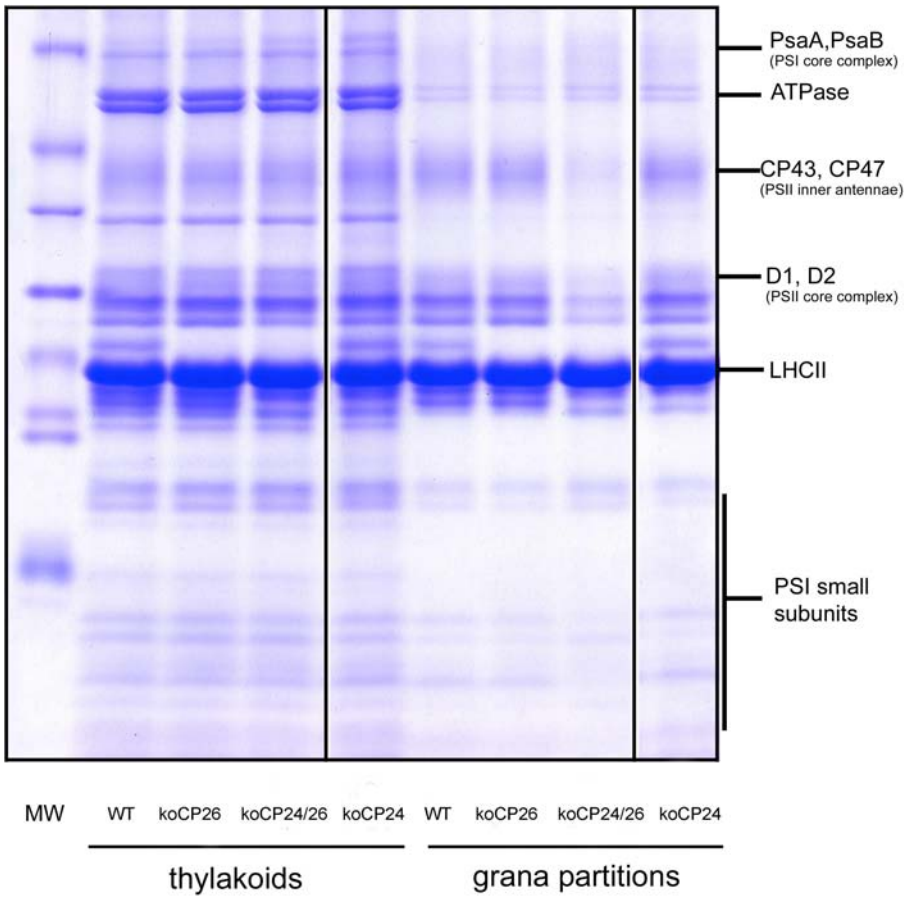

Supplemental Figure 3. Kinetics of plastoquinol re-oxidation upon exposure to far-red light. Details of Chl fluorescence traces described in Figure 11 shows decrease in stationary fluorescence (Fs) amplitude after oxidation of PQ obtained by turning on far-red light. Kinetics of Fs decrease depend on the rate of activation of kinase by reduced PQH_2.

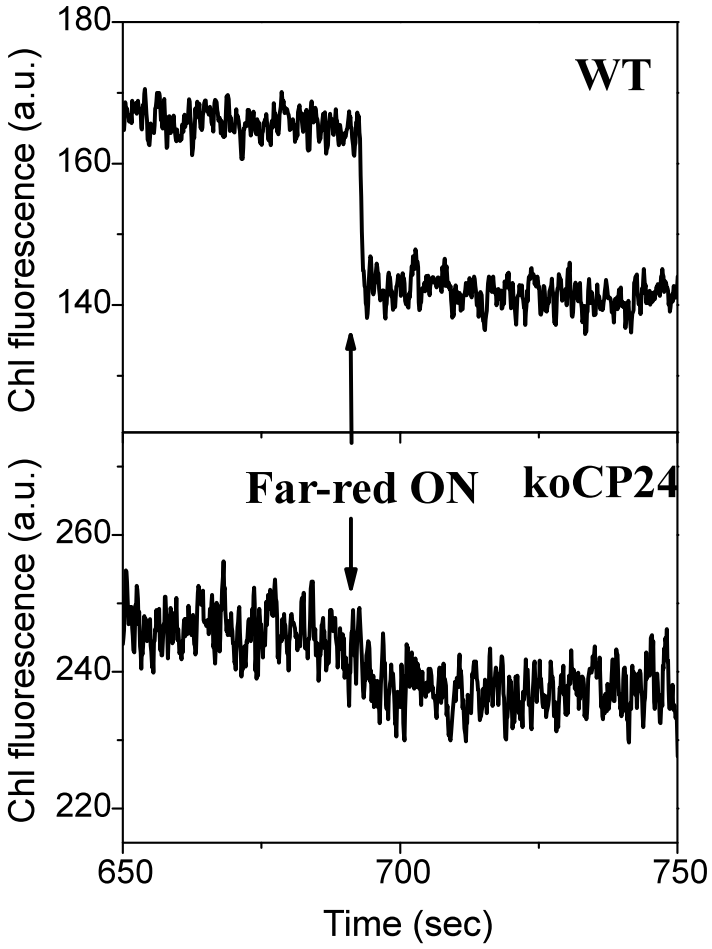

Supplemental Figure 4. Characterization of an additional allele for koCP24 (koCP24*lan*) establishes that this mutation is the only responsible of the observed phenotype. (A) Phenotype of wild type and mutant plants, grown in control conditions for four weeks (100 μmol photons m^{-2} s^{-1}, 25°C, 8/16 h d/n). (B) Kinetics of non-photochemical quenching (NPQ) induction and relaxation. Chlorophyll fluorescence was measured in intact, dark-adapted leaves, during 8 min of illumination at 1260 μmol m^{-2} s^{-1} followed by 9 min of dark relaxation. (C) Relative ETR as a function of quantum flux density of the photosynthetically active radiation (PAR), measured fluorometrically in light-adapted leaves under saturating CO_2 (1%). (D) PSII fluorescence induction kinetics normalized to the F_m value. (E) Q_A^- re-oxidation kinetics. Chl fluorescence decay kinetics were measured after single-turnover flash illumination in dark-adapted leaves. Drawn lines are fits for the experimental data points. Experimental fluorescence curves were normalized to the corresponding Fm values and represent averages from 12 separate experiments. (F) Measurement of state 1-state 2 transitions.

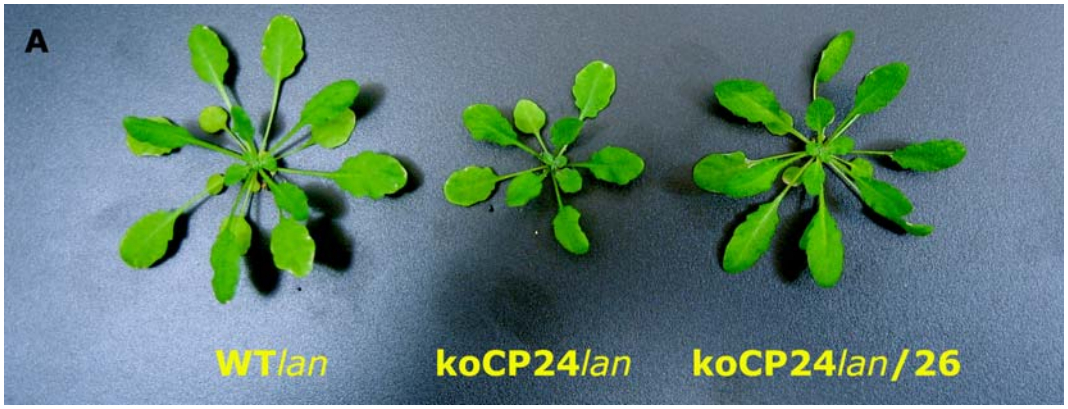
A
WTlan
koCP24lan
koCP24lan/26

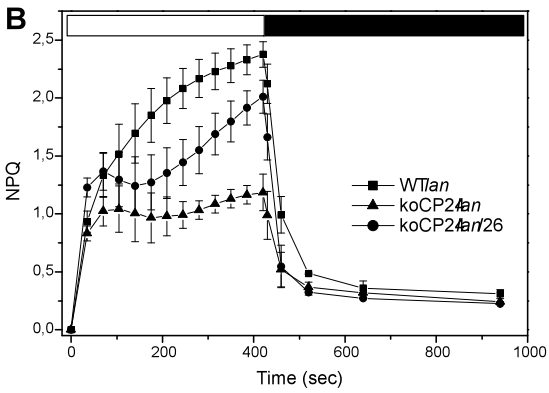
B
NPQ
Time (sec)
WTlan
koCP24lan
koCP24lan/26

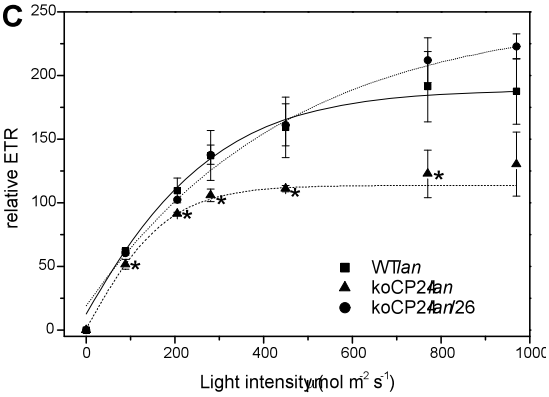
C
relative ETR
Light intensity (µmol m-2 s-1)
WTlan
koCP24lan
koCP24lan/26

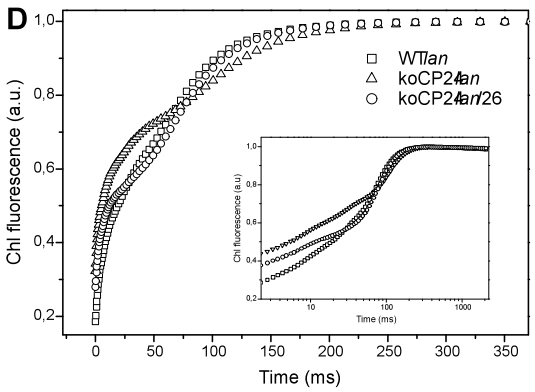
D
Chl fluorescence (a.u.)
Time (ms)
WTlan
koCP24lan
koCP24lan/26

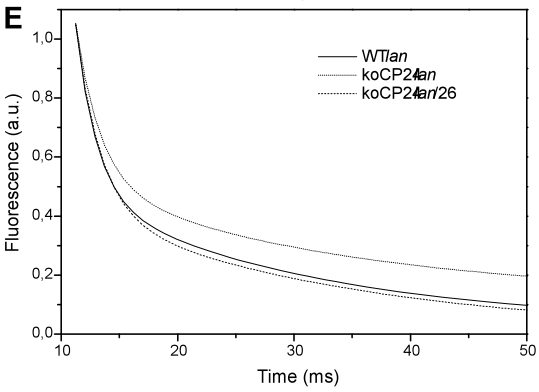
E
Fluorescence (a.u.)
Time (ms)
WTlan
koCP24lan
koCP24lan/26

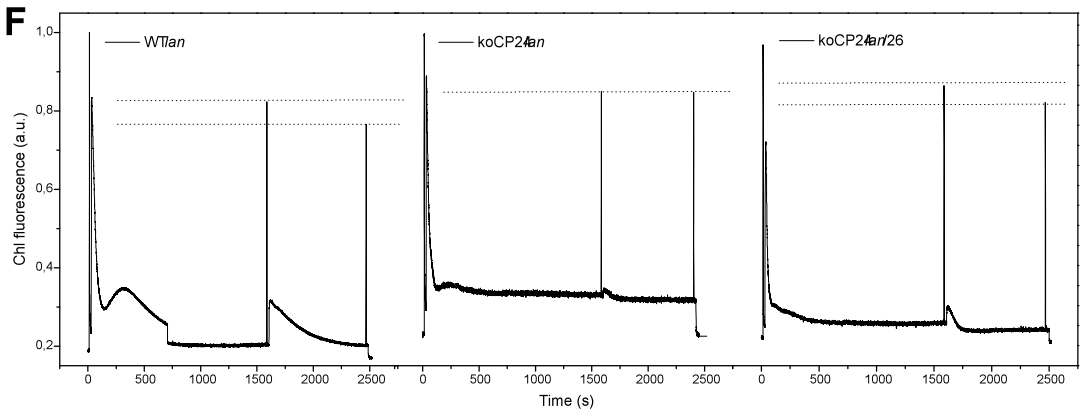
F
Chl fluorescence (a.u.)
Time (s)
WTlan
koCP24lan
koCP24lan/26

Supplemental Figure 5. **Chl fluorescence induction curves measured on grana membrane preparations from WT and koCP24 mutant.** The grana membrane preparation was also analyzed for fluorescence induction kinetics in order to verify that the functional features detected in leaves were actually present in the membrane preparation analyzed by electron microscopy. KoCP24 fluorescence rise was faster than WT in the O-I transition while it reached F_{max} at longer times than WT. Also the characteristics of koCP26 and koCP24/26 samples reproduced leaf results. In order to investigate if differences in Q_A re-oxidation kinetics were due to a higher average distance between PSII Q_B sites and cyt *b*$_6$*f* into the grana stacks, PSII membranes were treated with the cyt *b*$_6$*f* inhibitor DBMIB. Both WT and koCP24 grana samples exhibited a faster kinetic of fluorescence rise, i.e. Q_A reduction, in the presence of DBMIB with respect to their controls, implying some electron transport component (i.e. cyt b6/f) was blocked by the treatment. However, this effect was similar in both samples, suggesting no important differences in the distribution of this electron carrier were present in WT with respect to koCP24. Transient fluorescence rise was induced with a saturating green light (1100 µmol m^{-2} s^{-1}, 10 sec). Measurements were performed either in buffer solution (black, red traces) or in the presence of the Cyt *b*$_6$*f* inhibitor DBMIB 2 µM + ascorbate 25 mM (green, blue traces).

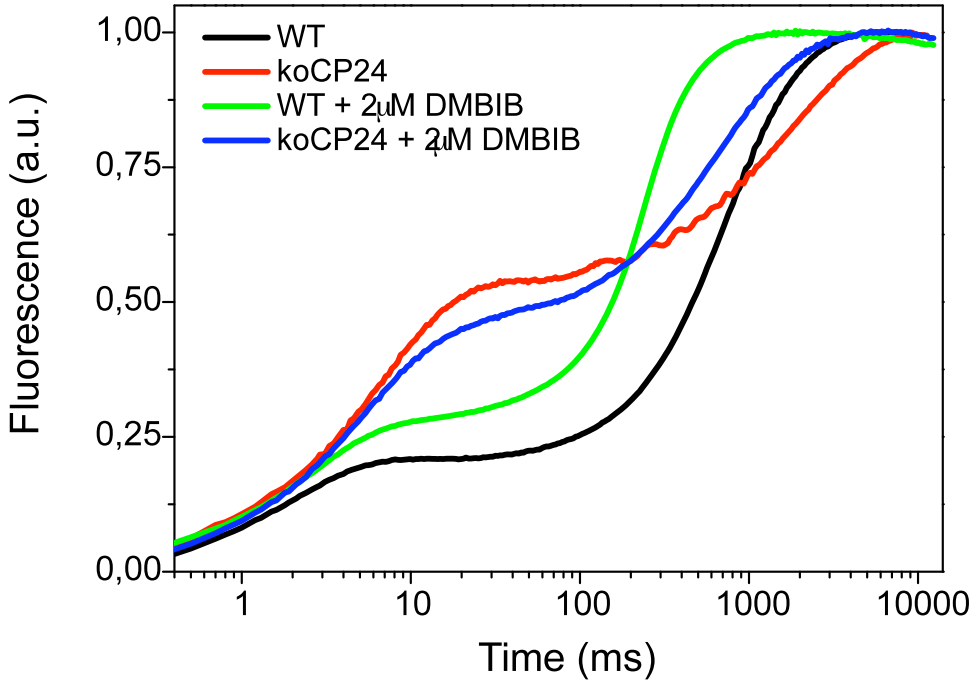

Supplemental Figure 6. Q_A^- re-oxidation kinetics. Chl fluorescence decay kinetics were measured after single-turnover flash illumination in dark-adapted leaves. The variable fluorescence decay, reflecting the re-oxidation of Q_A, was detected at 20 µs resolution. Experimental fluorescence curves were normalized to the corresponding Fm values and represent averages from 12 separate experiments.

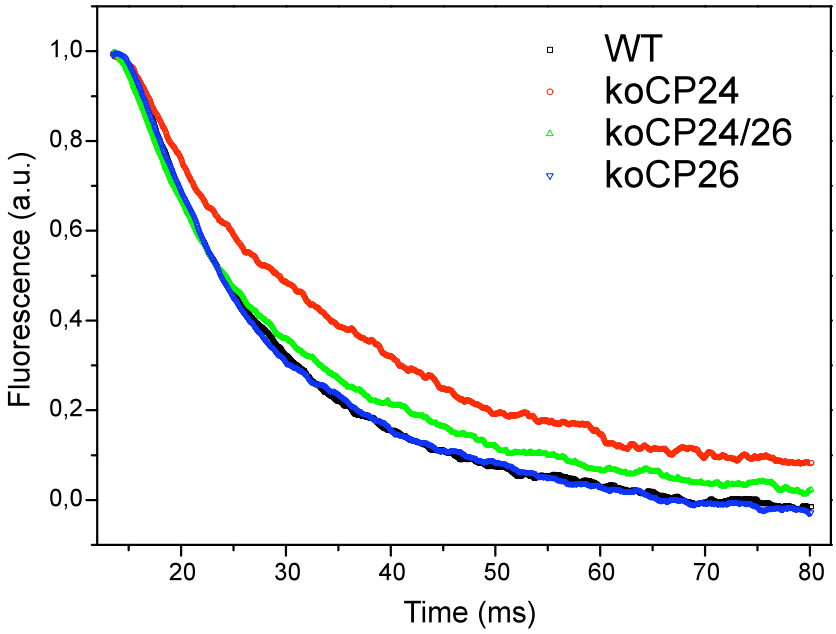

Supplemental Table 1. NPQ measurements on intact chloroplasts of WT and mutant genotypes. Maximum values of non-photochemical quenching (NPQ) were recorded with a PAM fluorometer. Chlorophyll fluorescence was measured in intact, dark-adapted chloroplasts, the same used for 9-AA quenching measurements. NPQ was induced during 6 min of illumination at 1260 μmol m^{-2} s^{-1} followed by 6 min of dark relaxation. All data are expressed as mean ± SD, n=3.

	WT	koCP24	koCP26	koCP24/26
NPQ	0.76 ± 0.21	0.41 ± 0.07	0.76 ± 0.07	0.68 ± 0.01